

# Supplementary Information: Delay-induced degrade-and-fire oscillations in small genetic circuits

William Mather, Matthew R. Bennett, Jeff Hasty, Lev S. Tsimring

(Dated: December 11, 2008)

## I. INTRODUCTION

This Supplementary Information is organized as follows. Section II introduces two models of delay-based degrade-and fire (DF) genetic oscillations in a single (negative feedback only) or dual (positive-negative feedback) systems. Section III contains the results of a deterministic analysis of the delayed negative feedback (NFB) system. Section IV examines stochastic oscillations in the NFB system and provides an analysis of the period variability due to stochastic effects. Section V briefly discusses a simplified version of the NFB-only system that uses a piecewise linear Hill function. Section VI discusses the effect of added positive feedback (PFB) on the degrade-and-fire oscillations.

## II. DELAYED FEEDBACK MODELS

The delayed negative feedback-only (NFB) oscillator is modeled by two reactions describing delayed birth and death processes for repressor protein. The rates  $K_+$  and  $K_-$  for production and degradation, respectively, of repressor  $r$  at the time  $t$  are

$$K_+(t) = F(r_\tau(t)) \quad (1)$$

$$K_-(t) = \frac{\gamma_r r(t)}{R_0 + r(t)} + \beta r(t) \quad (2)$$

$$F(r) \equiv \frac{\alpha}{\left(1 + \frac{r}{C_0}\right)^2}, \quad (3)$$

where the subscript  $\tau$  here and below denotes the value of a variable taken at time  $\tau$  before the current time  $t$ , i.e.  $r_\tau(t) = r(t - \tau)$ . Notice that a molecular derivation of the function  $F(r)$  may provide  $(1 + r/C_0)(1 + (r - 1)/C_0)$  instead of  $(1 + r/C_0)^2$ , but we use the latter for simplicity. Equations (1)-(3) can be simulated with a modified Gillespie algorithm [1], described previously [2].

We use a similar model for coupled positive-negative feedback (PNFB) which is inspired by our recent experimental study [3]. The rates  $K^{(r)}$  and  $K^{(a)}$  for repressor and activator, respectively, have the form

$$K_+^{(r)}(t) = F(r_\tau(t), a_\tau(t)) \quad (4)$$

$$K_-^{(r)}(t) = \frac{\gamma_r r(t)}{R_0 + r(t)} + \beta r(t) \quad (5)$$

$$K_+^{(a)}(t) = k F(r_{\tau_a}(t), a_{\tau_a}(t)) \quad (6)$$

$$K_-^{(a)}(t) = \frac{\gamma_a a(t)}{R_0 + a(t)} + \beta a(t) \quad (7)$$

$$F(r, a) \equiv \frac{\alpha \left(\frac{1}{f} + \frac{a}{C_1}\right)}{\left(1 + \frac{r}{C_0}\right) \left(1 + \frac{r}{C_0}\right)^2}, \quad (8)$$

where  $\tau_a$  is the delay time for the production of activator,  $k$  multiplies the production rate of activator, and  $f$  is a parameter characterizing the strength of positive feedback. The fully activated rate for repressor production is  $\alpha$ , while the corresponding basal rate (in the absence of activator) is  $\alpha/f$ . We do not include the coupling between the activator and repressor that arises between species degraded by a common protease, i.e. the coupling due to

competitive inhibition. The need for such degradation-based coupling arises in the modeling of systems like the synthetic oscillator describer in Ref. [3].

The effective treatment of dilution with a first order dilution rate  $\beta$  in the above models warrants a brief discussion. Dilution in the context of gene circuits is a reduction of the intracellular concentration of a species due to an increase in cell volume. For the corresponding deterministic systems, the  $\beta$ -terms for the degradation rates adequately model the effect of dilution. However, Eqs. (1)-(3) and (4)-(8) may not accurately predict the effect of dilution on species variability. A more realistic model of dilution treats cell volume  $V(t)$  as a time-dependent variable used to determine reaction rates, e.g. by replacing  $F(r(t))$  in Eqs. (1)-(3) with the scaled form  $V(t) F(r(t)/V(t))$ . The models given by Eqs. (1)-(3) and Eqs. (4)-(8) also do not include the effect of cell division when determining variability due to dilution; free intracellular components should be binomially distributed between daughter cells after each cell division.

### III. RESULTS FOR THE DETERMINISTIC NEGATIVE FEEDBACK-ONLY DF OSCILLATOR

In the deterministic limit, the NFB-only model (1)-(3) is described by the following delay-differential equation

$$\dot{r} = \frac{\alpha}{\left(1 + \frac{r_\tau}{C_0}\right)^2} - \frac{\gamma_r r}{R_0 + r} - \beta r. \quad (9)$$

In our analytical study, we take the limit  $R_0 \rightarrow 0$  and  $\beta \rightarrow 0$ , such that degradation occurs at the constant zero-order rate  $\gamma_r$ . Effects due to small  $R_0$  ( $R_0 \ll C_0$ ) do not seriously influence most of the results, e.g. the period, derived from Eq. (9), however they make analytical calculations (involving Lambert-W functions) more cumbersome. Effects due to small  $\beta$  ( $\beta\tau \ll 1$ ) are treated in Section III D.

The NFB model, Eq. (9), contains the basic mechanism for DF oscillations as described below. Notice that Eq. (9) can be integrated if the history of  $r(t)$  is known,

$$r(t) - r(t_i) = \int_{t_i - \tau}^{t - \tau} dt' \frac{\alpha}{\left(1 + \frac{r(t')}{C_0}\right)^2} - \gamma_r (t - t_i), \quad (10)$$

conditional on the solution remaining positive. Because of the limit  $R_0 \rightarrow 0$ , the case when  $r(t) = 0$  must be treated separately by forbidding  $r(t) < 0$  and by allowing  $r(t)$  to increase away from  $r(t) = 0$  when  $F(r_\tau(t)) > \gamma_r$ .

#### A. Linear stability analysis

Assuming  $\alpha > \gamma_r$ , the unique equilibrium point for Eq. (9) is given by the repressor value

$$r_{\text{on}} \equiv C_0 \left( \sqrt{\frac{\alpha}{\gamma_r}} - 1 \right). \quad (11)$$

Writing  $r(t) = r_{\text{on}} + \delta r(t)$ , for small  $\delta r(t)$ , a linearization of Eq. (9) leads to the delay-differential equation

$$\frac{d}{dt} \delta r = -\kappa \delta r_\tau, \quad (12)$$

with  $\kappa > 0$ . For the delayed negative feedback-only model,  $\kappa$  is readily calculated to be

$$\kappa = - \frac{\partial}{\partial r_\tau} \frac{\alpha}{\left(1 + \frac{r_\tau}{C_0}\right)^2} \Bigg|_{r=r_{\text{on}}} = \frac{2\alpha}{C_0 \left(1 + \frac{r_{\text{on}}}{C_0}\right)^3} = \frac{2}{C_0} \sqrt{\frac{\gamma_r^3}{\alpha}}. \quad (13)$$

The characteristic equation for Eq. (12) is

$$\lambda = -\kappa e^{-\lambda\tau}, \quad (14)$$

and it predicts instability when  $\text{Re} \lambda > 0$  for some solution to Eq. (14). It can be proved that this occurs only for sufficiently large  $\tau$  [4]. The instability condition is

$$\tau > \tau_c \equiv \frac{\pi}{2\kappa}, \quad (15)$$

where a supercritical Hopf bifurcation occurs, with the resulting period of the oscillations being  $4\tau$ . For our NFB-only system the instability condition can be written as

$$\tau > \frac{\pi C_0}{4} \sqrt{\frac{\alpha}{\gamma_r^3}}. \quad (16)$$

## B. Analysis of deterministic DF period

In this work we are interested in the strongly nonlinear regime of oscillations far above the Hopf bifurcation point defined by condition (16). In this regime, large oscillations arise (see Fig. 1 of the main text). These oscillations have a nearly triangular shape, with a steep rise of the repressor concentration in the beginning of each period followed by an almost linear decay back to zero after which the process repeats. We term these relaxation oscillations *degrade-and-fire* in analogy with integrate-and-fire oscillations in neuronal systems. The distinct two-phase regime of oscillations (rapid production phase and slow degradation phase) allows us to develop an analytical approach to deduce the properties of DF oscillations.

The most important first step in solving the problem is finding an approximate solution for the degradation phase, i.e. the times when repressor is slowly degrading after some previous burst of repressor. This is not a completely trivial task, but for large repressor concentration the production contribution can be neglected and for zero-order degradation we obtain

$$\dot{r} \approx -\gamma_r. \quad (17)$$

The approximate solution for the degradation phase is then given by

$$r(t) \approx -\gamma_r (t - t_0), \quad t_{\text{start}} \leq t \leq t_0, \quad (18)$$

where  $t_0$  is the time at which all repressor has been degraded to zero, and  $t_{\text{start}}$  is just after production of the previous pulse of repressor. The accuracy of the solution Eq. (18) can be improved by standard perturbative methods [5] (see Sec. III C). We will use the approximate solution Eq. (18) for further calculations.

After the repressor concentration becomes of the order of  $r_{\text{on}}$ , the production of new proteins begins, however due to delay they do not appear until time  $\tau$  later. Therefore, if  $\gamma_r \tau \gg r_{\text{on}}$ , one can neglect the new protein production throughout the degradation phase until the repressor concentration becomes zero at  $t = t_0$ . For  $t \geq t_0$ , repressor concentration  $r(t)$  remains at zero until the production rate of repressor  $F(r_\tau(t))$  exceeds the degradation rate  $\gamma_r$ . We call this the *principal production phase* since at this time the rate of production is maximal (equal to  $\alpha$ ). Define the time  $t_{\text{on}}$  by the condition  $r(t_{\text{on}}) = r_{\text{on}}$ , with  $r(t)$  from Eq. (18) and  $r_{\text{on}}$  from Eq. (11).  $t_{\text{on}}$  is the time when  $r(t)$  crosses the system's unstable equilibrium point, such that  $t_{\text{on}} + \tau$  is when the production rate of repressor exceeds the degradation rate. Thus,  $r(t) = 0$  for times in the range  $t_0 \leq t \leq t_{\text{on}} + \tau$ . Self-consistency requires that  $t_0 \leq t_{\text{on}} + \tau$ , which, using the above approximations, can be written  $\gamma_r \tau \geq r_{\text{on}}$ . That is, the time to degrade to zero from  $r_{\text{on}}$  should be less than the delay. In practice, the limit  $\gamma_r \tau \gg r_{\text{on}}$  may be used to assure self-consistency.

The solution for  $r(t)$  during times  $t_{\text{on}} + \tau \leq t \leq t_{\text{on}} + 2\tau$  depends on a solution for repressor at times  $t_{\text{on}} \leq t \leq t_{\text{on}} + \tau$  inserted in Eq. (10). The solution for times  $t_{\text{on}} \leq t \leq t_{\text{on}} + \tau$  was approximated in the preceding paragraphs. For times  $t_{\text{on}} + \tau < t < t_0 + \tau$ , Eq. (18) can be used to determine  $r(t)$ ,

$$r(t) \approx \frac{\alpha C_0}{\gamma_r} \left[ \left( 1 - \frac{(t - \tau) \gamma_r}{C_0} \right)^{-1} - \left( 1 - \frac{t_{\text{on}} \gamma_r}{C_0} \right)^{-1} \right] - \gamma_r (t - (t_{\text{on}} + \tau)), \quad t_{\text{on}} + \tau \leq t \leq t_0 + \tau. \quad (19)$$

Similarly, the solution for times  $t_0 + \tau \leq t \leq t_{\text{on}} + 2\tau$  can be written as

$$r(t) \approx r(t_0 + \tau) + (\alpha - \gamma_r)(t - t_0 - \tau), \quad t_0 + \tau \leq t \leq t_{\text{on}} + 2\tau, \quad (20)$$

where  $r(t_0 + \tau)$  is obtained from Eq. (19).

Because  $r(t)$  is now known for times  $t \leq t_{\text{on}} + 2\tau$ , we can continue to use Eq. (10) over the solutions in Eqs. (19) and (20). In integral form we arrive at

$$r(t) = r(t_{\text{on}} + 2\tau) + \int_{t_{\text{on}} + \tau}^{t - \tau} dt' \frac{\alpha}{\left(1 + \frac{r(t')}{C_0}\right)^2} - \gamma_r (t - (t_{\text{on}} + 2\tau)), \quad t_{\text{on}} + 2\tau \leq t \leq t_{\text{on}} + 3\tau. \quad (21)$$

This solution can be expressed in terms of elementary functions, although this expression is rather cumbersome. Since  $r(t) \gg C_0$  for  $t_{\text{on}} + 2\tau \leq t \leq t_{\text{on}} + 3\tau$ , repressor is no longer being produced in significant quantities by time  $t_{\text{on}} + 3\tau$ . Thus, a new degradation phase has begun at time  $t_{\text{on}} + 3\tau$ , and we have approximately solved for the trajectory  $r(t)$  over one period of oscillation.

The period of oscillations,  $T$ , is composed of the time to produce a burst of  $P$  repressor proteins ( $t_{\text{on}} + 3\tau - t_0$ ) and the time to degrade it  $P/\gamma_r$ . Thus,

$$T = \frac{P}{\gamma_r} + (t_{\text{on}} + 3\tau - t_0). \quad (22)$$

Here we define  $P$  as

$$P \equiv r(t_{\text{on}} + 3\tau). \quad (23)$$

During the principal production phase, defined by when  $r(t) = 0$  during  $t_0 \leq t \leq t_{\text{on}} + \tau$ , the Hill function  $\alpha/(1 + r/C_0)^2$  attains its maximum value  $\alpha$ . The increase of repressor  $P_0$  due to production from this phase (actual production occurs a time  $\tau$  later) is given by

$$P_0 = r(t_{\text{on}} + 2\tau) - r(t_0 + \tau) = (\alpha - \gamma) (t_{\text{on}} + \tau - t_0), \quad (24)$$

or, by previous estimates,

$$P_0 \approx (\alpha - \gamma) \left( \tau - \frac{r_{\text{on}}}{\gamma} \right) = (\alpha - \gamma) \left[ \tau - \frac{C_0}{\gamma} \left( \sqrt{\frac{\alpha}{\gamma}} - 1 \right) \right]. \quad (25)$$

$P_0$  provides the dominant contribution to the amplitude and period of NFB-only oscillations when  $t_{\text{on}} - t_0 \ll \tau$ , i.e. when  $\tau$  is long relative to the time to degrade from  $r_{\text{on}}$ .

A simpler but less accurate formula for the period can be constructed. We suppose that a pulse of repressor takes a time  $2\tau$  to be created, since repressor typically peaks around the time  $t_0 + 2\tau$ . Also, the production  $P$  in Eq. (23) is often well approximated by its principal part  $P_0$  in Eq. (25) if  $\gamma_r \tau \gg r_{\text{on}}$ . A simpler estimate for the period is then

$$T_0 = \frac{P_0}{\gamma_r} + 2\tau. \quad (26)$$

Equation (26) reproduces many of the features of numerical period data from direct numerical integration of Eq. (9), including a period maximum as  $\gamma_r$  or  $\alpha$  is varied. Equation (26) also reproduces the exact  $C_0 \rightarrow 0$  result for the period.

### C. Corrections for the degradation phase of DF oscillations

When the inequality  $\gamma_r \tau \gg r_{\text{on}}$  is satisfied, a perturbation series solution for the degradation phase may be expected. This perturbation expansion is found by scaling  $\alpha \rightarrow \epsilon \alpha$ , i.e. by assuming production is small. The formal solution for the repressor trajectory is written as the series

$$r(t) = \sum_{n=0}^{\infty} \epsilon^n r_n(t). \quad (27)$$

We insert Eq. (27) into Eq. (9) with  $R_0 = 0$ ,  $\beta = 0$ , and Taylor expansion of  $F(r)$  in the variable  $\epsilon$ . The perturbation expansion can be generated by identifying terms of same  $\epsilon$  order in the equation

$$\sum_{n=0}^{\infty} \epsilon^n \dot{r}_n(t) = \epsilon \sum_{m=0}^{\infty} \frac{1}{m!} \frac{d^m F}{dr^m}(r_0(t-\tau)) \left( \sum_{n=1}^{\infty} \epsilon^n r_n(t-\tau) \right)^m - \gamma_r. \quad (28)$$

The lowest order equation is

$$\dot{r}_0(t) = -\gamma_r, \quad (29)$$

i.e. Eq. (17). The perturbation series solution is straightforward for low orders. These lowest order terms are

$$r_0(t) = -\gamma_r(t - \tilde{t}_0) \quad (30)$$

$$r_1(t) = \frac{\alpha C_0^2}{\gamma_r} \frac{1}{C_0 - \gamma_r(t - \tilde{t}_0 - \tau)} \quad (31)$$

$$r_2(t) = \frac{\alpha^2 C_0^4}{\gamma_r^5 \tau^3} \left[ \gamma_r \tau \frac{2C_0 - \gamma_r(2t - 2\tilde{t}_0 - \tau)}{(C_0 - \gamma_r(t - \tilde{t}_0 - \tau))^2} - 2 \ln \left( \frac{C_0 - \gamma_r(t - \tilde{t}_0 - 2\tau)}{C_0 - \gamma_r(t - \tilde{t}_0 - \tau)} \right) \right], \quad (32)$$

where the zeroth order solution is set to zero at time  $t = \tilde{t}_0$ .  $\tilde{t}_0$  is thus the lowest order approximation to the true time  $t_0$ . An estimate of the correction to the zeroth order solution used in Section III B is the value of the first correction at  $t = \tilde{t}_0$ ,

$$r_1(\tilde{t}_0) = \frac{\alpha}{\gamma_r} \frac{C_0^2}{C_0 + \gamma_r \tau}, \quad (33)$$

which is much less than order  $C_0$  when  $\gamma_r \tau \gg C_0 [(\alpha/\gamma_r) - 1]$ . This condition can be compared to the condition  $\gamma_r \tau \gg C_0 [\sqrt{\alpha/\gamma_r} - 1]$  that was used in the derivation of the period in Section III B.

Note that the perturbation series solution should more appropriately be taken to end before the time  $t^* = t_0 - r_{\text{on}}/\gamma_r$ , i.e. when  $r_0(t^*) = r_{\text{on}}$  (the fixed point of Eq. (9)). Such a procedure can be used if the perturbation expansion fails to produce accurate results at times near  $t_0$ .

#### D. Corrections for small $\beta$

The effects of dilution due to cell growth were excluded in the preceding analysis by setting  $\beta = 0$ . However, dilution effects may become important when the cell division period is sufficiently short to be comparable to the oscillation period. We discuss here the small  $\beta$  effects in the negative feedback-only oscillator.

Suppose that dilution is weak on the timescale  $\tau$  of production, i.e.

$$\beta \tau \ll 1. \quad (34)$$

In this case, Eq. (34) ensures that the relative change in  $r(t)$  due to dilution remains small over a time  $\tau$ . The condition Eq. (34) allows dilution to be neglected during the time  $\approx 2\tau$  taken to produce a burst of repressor. Thus, the magnitude  $P$  for a burst of repressor for a system with small  $\beta$  is essentially equal to the  $\beta = 0$  result.

The degradation of a pulse of magnitude  $P$  can be strongly affected by dilution. The repressor degradation phase trajectory follows from the solution of Eq. (9) when production is negligible,

$$r(t) = -\frac{\gamma_r}{\beta} + e^{-\beta(t-t_{\text{start}})} \left( P + \frac{\gamma_r}{\beta} \right), \quad (35)$$

where  $t = t_{\text{start}}$  is the time when degradation phase of the pulse begins. The time,  $T_D(\beta)$ , for  $r(t)$  to degrade to zero is then given by

$$\beta T_D(\beta) = \ln(1 + \beta T_D(0)), \quad (36)$$

where  $T_D(0) = P/\gamma_r$ . Thus, dilution has a negligible effect on the oscillation period when  $\beta T_D(0) \ll 1$ , i.e. when cell division is slow relative to the  $\beta = 0$  oscillation period.

### E. Nonlinearity and the robustness of oscillations

For this study, the exponent  $n$  in the production rate  $\alpha/(1+r_\tau/C_0)^n$  was chosen to be 2, which is a realistic value for gene regulatory systems. However,  $n$  need not be 2, and its value will affect the robustness of degrade and fire oscillations. In general,  $n$  should be sufficiently large for robust degrade-and-fire oscillations to occur. Fig. 1 presents results for the NFB-only oscillator that illustrate this relationship. The region of parameter space that supports oscillations is here seen to increase with increasing  $n$ . That is, high  $n$  leads to robustness of oscillations against variability in system parameters. Such variability naturally occurs across a population of biological cells, and hence, physical gene circuits should possess the quality of robustness for consistent operation across a population. In addition to robustness, higher  $n$  supports degrade-and-fire oscillations more readily than lower values of  $n$ . Both of these observations suggest high nonlinearity (large  $n$ ) is associated with robust degrade-and-fire oscillations in physical gene circuits.

The importance of nonlinearity can be further illustrated by a related nearly-linear oscillator. The above systems can be linearized about their fixed point  $r_0$  to provide the linear delay differential equation

$$\frac{dr}{dt} = b_1(r - r_0) + b_2(r_\tau - r_0) \quad (37)$$

where  $b_1$  and  $b_2$  are the linear coefficients

$$b_1 = -\left. \frac{\partial}{\partial r} \frac{\gamma r}{R_0 + r} \right|_{r=r_0} = -\frac{\gamma R_0}{(R_0 + r_0)^2} \quad (38)$$

$$b_2 = \left. \frac{\partial}{\partial r} \frac{\alpha}{(1 + r/C_0)^n} \right|_{r=r_0} = -\frac{n\alpha}{C_0(1 + r_0/C_0)^{n+1}} \quad (39)$$

We augment this linear system with the condition  $r(t) \geq 0$ , as done elsewhere in this text, such that growing oscillations remain finite in amplitude. This nearly-linear system has the same bifurcation diagram as the corresponding systems in Fig. 1a, but the period relative to  $\tau$  is now decreasing with increasing  $\tau$  (ref. Fig. 1b-c). This can be contrasted against the long-period oscillations that are generated through degrade-and-fire dynamics.

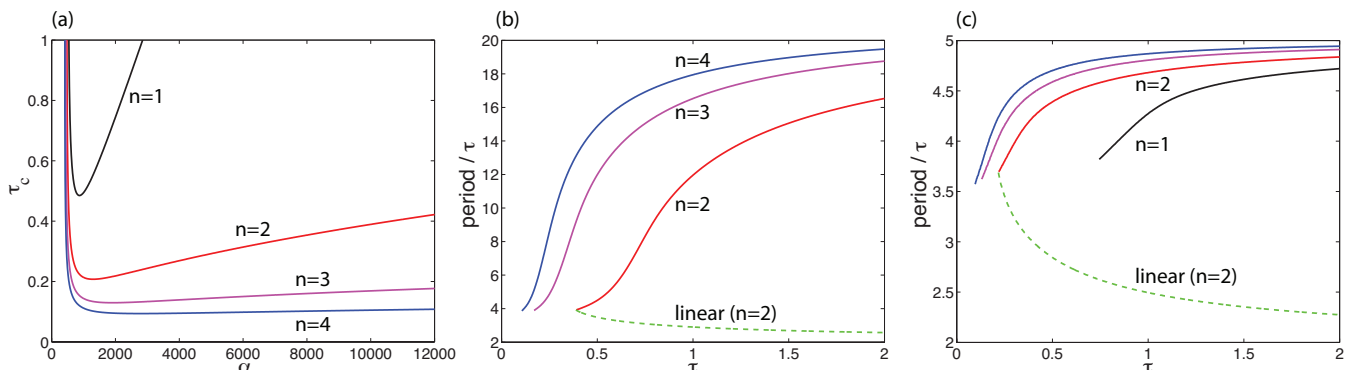


FIG. 1: (a) Plot of the critical period  $\tau_c$  vs.  $\alpha$  for the deterministic NFB-only system, with  $C_0 = 50$ , enzymatic degradation constants  $\gamma = 500$  and  $R_0 = 10$ , and variable  $n$  (labeled in plot). The fixed point of the system is unstable to oscillations when  $\tau > \tau_c$ . (b) Plot of period (in units of  $\tau$ ) vs.  $\tau$  for the systems in part (a), with  $\alpha = 10000$ . Each period curve terminates at the lower value  $\tau = \tau_c$ . Results are also presented for the nearly-linear oscillator (with  $n = 2$ , as described in the text of Section III E). (c) Similar to (b), but with  $\alpha = 2000$ .

## IV. STOCHASTIC NEGATIVE FEEDBACK-ONLY OSCILLATOR

While deterministic equations are useful in understanding the behavior of gene circuits, variability of gene expression is an essential aspect not contained in the deterministic equations. Molecular events, including production and degradation of protein, occur in a seemingly random fashion within a cell [6]. This so-called intrinsic noise leads to variability of the amplitude and period of DF oscillations.

In this Section we analyze the amplitude and period of DF oscillations for the stochastic NFB system with  $R_0 \rightarrow 0$  and  $\beta\tau \ll 1$  based on the full stochastic system described by Eqs. (1)-(3). The stochastic trajectories, like their deterministic counterparts, can be decomposed into brief production phases when a burst of repressor production occurs and relatively long periods of its subsequent degradation (Sec. IV A). The condition  $\gamma_r\tau \gg r_{\text{on}}$  is again assumed, such that repressor reaches  $r = 0$  during the production phases with high probability.

This section neglects the effects of mRNA dynamics. Because multiple proteins tend to be translated off of a single mRNA, the fluctuations associated with protein production are largely determined by mRNA fluctuations. Many of the effects of mRNA variability can be determined with only minor modifications to the present analysis, namely, by enhancing the variability associated with production of a given number of repressor proteins.

As a matter of notation for the following, the variance of a random variable  $A$  is written  $\langle \Delta A^2 \rangle \equiv \langle A^2 \rangle - \langle A \rangle^2$ . We also use the correlation operator  $\kappa(x_1, x_2) \equiv \langle x_1 x_2 \rangle - \langle x_1 \rangle \langle x_2 \rangle$  for two random variables  $x_1$  and  $x_2$ .

This section is broken into several parts. Section IV A discusses how period and amplitude variance are related. Section IV B explains how to approximate amplitude variance. Section IV C presents numerical results.

### A. Period variability and its relationship to amplitude variability

The production phase of repressor is defined to occur during a fixed time  $T_P$  after the burst of repressor produced during a previous oscillation period first degrades to zero. Without losing generality, we synchronize stochastic trajectories at the beginning of the production phase, i.e. so the number of repressor molecules becomes zero at a fixed (non-fluctuating) time  $t_0$ . We define the duration of the production phase deterministically as  $T_P = t_{\text{on}} - t_0 + 3\tau$ . However, the amplitude at the end of the production phase  $P = r(t_0 + T_P)$  is random. The time  $T_D(\beta)$  for repressor to degrade back to zero depends on  $P$  and is thus also random. The total period for this oscillation is  $T = T_P + T_D(\beta)$ . Thus, the period variance  $\langle \Delta T^2 \rangle = \langle \Delta T_D(\beta)^2 \rangle$ .

To compute  $\langle \Delta T_D^2 \rangle$ , we assume first that  $P$  is sharply distributed and later average over  $P$  to provide the result for random  $P$ . If production can be ignored, the time to degrade to zero conditional on starting at  $P$  is a sum of exponentially distributed and independent times  $\Delta t_n$  (see Eqs. (1)-(3)),

$$T_D(\beta) = \sum_{n=1}^P \Delta t_n, \quad (40)$$

with average

$$\langle \Delta t_n \rangle = \frac{1}{\gamma_r + \beta n} \quad (41)$$

and correlation

$$\kappa(\Delta t_n, \Delta t_m) = \delta_{n,m} \langle \Delta t_n \rangle^2, \quad (42)$$

where  $\delta_{n,m}$  is the Kronecker delta function. From Eq. (42), one can show

$$\langle T_D(\beta) \rangle = \sum_{n=1}^P \langle \Delta t_n \rangle \quad (43)$$

$$\langle T_D(\beta)^2 \rangle = \sum_{n=1}^P \langle \Delta t_n \rangle^2 + \langle T_D(\beta) \rangle^2, \quad (44)$$

provided  $P$  is fixed. Equations (43) and (44) can be expressed in terms of polygamma functions for the value of  $\langle \Delta t_n \rangle$  given by Eq. 41. For  $\beta = 0$ , the expressions are

$$\langle T_D(\beta) \rangle = \frac{P}{\gamma_r} \quad (45)$$

$$\langle T_D(\beta)^2 \rangle = \frac{P}{\gamma_r^2} + \frac{P^2}{\gamma_r^2}. \quad (46)$$

The case  $\beta > 0$  can be treated approximately. For example, if  $\beta \ll \gamma_r$  and  $P \gg 1$ , the sum in  $\langle T_D(\beta) \rangle$  may be approximated by the integral

$$\langle T_D(\beta) \rangle = \sum_{n=1}^P \langle \Delta t_n \rangle \approx \int_0^P dn \left\langle \frac{1}{\gamma_r + \beta n} \right\rangle = \frac{1}{\beta} \ln \left( 1 + \frac{\beta P}{\gamma_r} \right) = \frac{1}{\beta} \ln (1 + \beta \langle T_D(0) \rangle), \quad (47)$$

which is identical to the deterministic result. More accurate approximations for  $\langle \Delta T_D(\beta) \rangle$  and  $\langle \Delta T_D(\beta)^2 \rangle$  can be derived by application of the Euler-Maclaurin formula.

Since the burst magnitude  $P$  is random, Eqs. (43) and (44) must be averaged over  $P$ . In the case  $\beta = 0$ , the calculations are tractable, with the result for the period variance given by

$$\langle \Delta T_D(\beta = 0)^2 \rangle = \frac{\langle P \rangle}{\gamma_r^2} + \frac{\langle \Delta P^2 \rangle}{\gamma_r^2}. \quad (48)$$

The first term on the r.h.s. of Eq. (48) is due to inherent variability of the degradation process; this term is present even when  $P$  is sharply defined. The second term is proportional to the variance of the pulse amplitude  $P$ . Thus, the period variance can be determined directly from the burst amplitude variance  $\langle \Delta P^2 \rangle$  when  $\beta = 0$ . We do not present results for  $\langle \Delta T_D(\beta)^2 \rangle$  in the  $\beta > 0$  case, though their derivation is straightforward.

## B. Analysis of pulse amplitude variance

This section outlines how to compute the repressor pulse amplitude variance  $\langle \Delta P^2 \rangle$ , which is used in Eq. (48) to determine the period variance. Our analysis of the pulse amplitude variance depends on integration of the stochastic system for a small time duration, starting from the time  $t_0$  when  $r(t) = 0$  first occurs and ending a time  $T_P = t_{\text{on}} - t_0 + 3\tau$  later (the duration  $t_{\text{on}} - t_0$  is defined by the deterministic system).

Section IV B 1 presents equations that will be used in the analysis of stochastic repressor dynamics. The remaining Sections IV B 2-IV B 4 apply the results of Section IV B 1 to particular time intervals of the repressor trajectory.

### 1. Probability evolution for repressor trajectories

The stochastic system with the rates in Eq. (1)-(3) can be analyzed in terms of its master equation [7]. Suppose that a particular stochastic history  $r(t)$  is taken for times  $t_i - \tau \leq t \leq t_i$ , the evolution of the probability distribution of repressor, conditional on the history, obeys for times  $t_i \leq t \leq t_i + \tau$

$$\dot{p}_n(t) = K_+(t) p_{n-1}(t) + K_-(t) p_{n+1}(t) - (K_+(t) + K_-(t)) p_n(t) \quad , \quad n \geq 1 \quad (49)$$

$$\dot{p}_0(t) = K_-(t) p_1(t) - K_+(t) p_0(t), \quad (50)$$

where the functions  $K_+(t)$  and  $K_-(t)$  are functions of  $r_\tau(t)$ . The full statistics of  $r(t)$  for times  $t_i \leq t \leq t_i + \tau$ , conditional on  $r(t)$  for times  $t_i - \tau \leq t \leq t_i$ , can be derived from Eqs. (49) and (50). Similarly, given the full statistics of all histories  $r(t)$  for times  $t_i - \tau \leq t \leq t_i$  (including multi-time correlation functions), the statistics of  $r(t)$  for times  $t_i \leq t \leq t_i + \tau$  conditional on these histories can be found by averaging results from Eqs. (49) and (50) over all histories. In principle, this procedure can be iterated to integrate the system to distant future times. In practice, however, this procedure can quickly become complicated. Our goal in this section is to derive from the above procedure a practical method to calculate  $\langle \Delta P^2 \rangle$  for the NFB system.

Solutions to Eqs. (49) and (50) for known time-dependent rates  $K_+(t)$  and  $K_-(t)$  are made difficult by the qualitative change in behavior at  $r = 0$  due to a ‘‘reflecting boundary.’’ This difficulty is removed if we ignore the reflecting boundary by assuming  $p_0(t)$  is essentially zero for  $t_i \leq t \leq t_i + \tau$ . Notice that this assumption for repressor to be above zero need not apply to the histories  $r(t)$  for times  $t_i - \tau \leq t \leq t_i$ . For the remainder of Section IV B 1, we suppose  $p_0(t) = 0$  for  $t_i \leq t \leq t_i + \tau$ . Sections IV B 2-IV B 4 will handle separately the case when  $p_0(t)$  may be large.

First, consider the situation where a particular history  $r(t)$  is taken for times  $t_i - \tau \leq t \leq t_i$ , such that  $K_+(t)$  and

$K_-(t)$  are known functions of time. Assuming  $p_0(t) = 0$ , with the help of the generating function

$$G(s, t) = \sum_{n=0}^{\infty} s^n p_n, \quad (51)$$

Eqs. (49) and (50) can be recast in the form

$$\dot{G}(s, t) = [(s-1)K_+(t) + (s^{-1}-1)K_-(t)] G(s, t). \quad (52)$$

Equation (52) has as its solution

$$G(s, t) = G(s, t_i) \exp \int_{t_i}^t dt' [(s-1)K_+(t') + (s^{-1}-1)K_-(t')]. \quad (53)$$

From Eq. (53) one can derive the first and second moments,

$$\begin{aligned} \langle r(t) \rangle &= \sum_{n=0}^{\infty} n p_n(t) = \frac{\partial G}{\partial s}(1, t) = \langle r(t_i) \rangle + \int_{t_i}^t dt' v(t') \\ \langle r(t)^2 \rangle &= \sum_{n=0}^{\infty} n^2 p_n(t) = \left[ \frac{\partial}{\partial s} s \frac{\partial}{\partial s} G(s, t) \right]_{s=1} \\ &= \langle r(t_i)^2 \rangle + \int_{t_i}^t dt' B(t') + 2 \langle r(t_i) \rangle \int_{t_i}^t dt' v(t') + \int_{t_i}^t dt'_2 \int_{t_i}^{t'_2} dt'_1 v(t'_2) v(t'_1), \end{aligned} \quad (54)$$

where we have defined

$$\begin{aligned} B(t) &\equiv K_+(t) + K_-(t), \\ v(t) &\equiv K_+(t) - K_-(t). \end{aligned} \quad (55)$$

The two-time average  $\langle r(t_2)r(t_1) \rangle$  is derived similarly, with result

$$\begin{aligned} \langle r(t_2)r(t_1) \rangle &= \langle r(t_1)^2 \rangle + \langle r(t_1) \rangle \int_{t_1}^{t_2} dt' v(t') \\ &= \langle r(t_i)^2 \rangle + \int_{t_i}^{t_1} dt' B(t') + \langle r(t_i) \rangle \int_{t_i}^{t_1} dt' v(t') + \langle r(t_i) \rangle \int_{t_i}^{t_2} dt' v(t') \\ &\quad + \int_{t_i}^{t_2} dt'_2 \int_{t_i}^{t'_2} dt'_1 v(t'_2) v(t'_1), \end{aligned} \quad (56)$$

with  $t_i + \tau \geq t_2 \geq t_1 \geq t_i$ . Again, each of these results are conditional on a given history  $r(t)$ , such that we can replace  $\langle r(t_i) \rangle = r(t_i)$  and  $\langle r(t_i)^2 \rangle = r(t_i)^2$ ,

$$\langle r(t) \rangle = r(t_i) + \int_{t_i}^t dt' v(t') \quad (57)$$

$$\begin{aligned} \langle r(t_2)r(t_1) \rangle &= r(t_i)^2 + \int_{t_i}^{t_1} dt' B(t') + r(t_i) \int_{t_i}^{t_1} dt' v(t') + r(t_i) \int_{t_i}^{t_2} dt' v(t') \\ &\quad + \int_{t_i}^{t_2} dt'_2 \int_{t_i}^{t'_2} dt'_1 v(t'_2) v(t'_1). \end{aligned} \quad (58)$$

To evolve a set of trajectories generated by the stochastic system, Eqs. (57) and (58) must be averaged over all previous histories. Now using angular brackets  $\langle \cdot \rangle$  that also average over histories, the averaged Eqs. (57) and (58) can be written in the form

$$\langle r(t) \rangle = \langle r(t_i) \rangle + \int_{t_i}^t dt' \langle v(r_\tau(t')) \rangle \quad (59)$$

$$\begin{aligned} \kappa(r(t_2), r(t_1)) &= \kappa(r(t_i), r(t_i)) + \int_{t_i}^{t_1} dt' \langle B(r_\tau(t')) \rangle + \int_{t_i}^{t_1} dt' \kappa(r(t_i), v(r_\tau(t'))) + \int_{t_i}^{t_2} dt' \kappa(r(t_i), v(r_\tau(t'))) \\ &\quad + \int_{t_i}^{t_2} dt'_2 \int_{t_i}^{t'_2} dt'_1 \kappa(v(r_\tau(t'_2)), v(r_\tau(t'_1))), \end{aligned} \quad (60)$$

where  $\kappa$  is the correlation operator. The last three terms on the r.h.s. of Eq. (60) are due to delayed interactions and involve two-time correlation functions of nonlinear functions of the history  $r(t)$ .

Equations (59) and (60) do not give  $\langle r(t) \rangle$  and  $\kappa(r(t_2), r(t_1))$  in terms of their previous values. For example, Eq. (60) requires the two-time correlation of the nonlinear function  $v(r)$ , which in turn may be expressed in terms of the correlations  $\kappa(r^n(t_2), r^m(t_1))$  for  $n, m$  integers greater than zero. This issue can be addressed with perturbative “small-noise” expansions. We write the repressor trajectory as a mean part plus a small variable part  $r(t) = \langle r(t) \rangle + \delta r(t)$ , with  $\langle \delta r(t) \rangle = 0$ . After Taylor expanding the functions  $v(r)$  and  $B(r)$  with respect to  $\delta r$  and substituting in Eqs. (59), (60), we find to second order in  $\delta r$ :

$$\begin{aligned} \langle r(t) \rangle &\approx \langle r(t_i) \rangle + \int_{t_i}^t dt' \left( v(\langle r_\tau(t') \rangle) + \frac{1}{2} \frac{\partial^2 v}{\partial r^2}(\langle r_\tau(t') \rangle) \langle \Delta r(t')^2 \rangle \right) \\ \kappa(r(t_2), r(t_1)) - \kappa(r(t_i), r(t_i)) &\approx \int_{t_i}^{t_1} dt' \left( B(\langle r_\tau(t') \rangle) + \frac{1}{2} \frac{\partial^2 B}{\partial r^2}(\langle r_\tau(t') \rangle) \langle \Delta r(t')^2 \rangle \right) \\ &\quad + \int_{t_i}^{t_1} dt' \frac{\partial v}{\partial r}(\langle r_\tau(t') \rangle) \kappa(r(t_i), r_\tau(t')) + \int_{t_i}^{t_2} dt' \frac{\partial v}{\partial r}(\langle r_\tau(t') \rangle) \kappa(r(t_i), r_\tau(t')) \\ &\quad + \int_{t_i}^{t_2} dt'_2 \int_{t_i}^{t_1} dt'_1 \frac{\partial v}{\partial r}(\langle r_\tau(t'_2) \rangle) \frac{\partial v}{\partial r}(\langle r_\tau(t'_1) \rangle) \kappa(r_\tau(t'_2), r_\tau(t'_1)) \end{aligned} \quad (61)$$

with  $t_i \leq t_1 \leq t_2 \leq t_i + \tau$  and with averages are over  $\delta r(t)$ . Note that  $\kappa(r(t_2), r(t_1)) = \kappa(\delta r(t_2), \delta r(t_1))$ . Assuming the terms  $\langle \delta r(t)^2 \rangle$  and  $B(r)$  are both “small”, we neglect the correction proportional to  $\frac{\partial^2 B}{\partial r^2}(\langle r_\tau(t') \rangle) \langle \Delta r(t')^2 \rangle$  to give

$$\begin{aligned} \langle r(t) \rangle &\approx \langle r(t_i) \rangle + \int_{t_i}^t dt' \left( v(\langle r_\tau(t') \rangle) + \frac{1}{2} \frac{\partial^2 v}{\partial r^2}(\langle r_\tau(t') \rangle) \langle \Delta r(t')^2 \rangle \right) \\ \kappa(r(t_2), r(t_1)) - \kappa(r(t_i), r(t_i)) &\approx \int_{t_i}^{t_1} dt' B(\langle r_\tau(t') \rangle) \\ &\quad + \int_{t_i}^{t_1} dt' \frac{\partial v}{\partial r}(\langle r_\tau(t') \rangle) \kappa(r(t_i), r_\tau(t')) + \int_{t_i}^{t_2} dt' \frac{\partial v}{\partial r}(\langle r_\tau(t') \rangle) \kappa(r(t_i), r_\tau(t')) \\ &\quad + \int_{t_i}^{t_2} dt'_2 \int_{t_i}^{t_1} dt'_1 \frac{\partial v}{\partial r}(\langle r_\tau(t'_2) \rangle) \frac{\partial v}{\partial r}(\langle r_\tau(t'_1) \rangle) \kappa(r_\tau(t'_2), r_\tau(t'_1)). \end{aligned} \quad (63)$$

Equations (62) and (63) generate mean values and correlation functions of  $r(t)$  in terms of their previous values, as needed.

The lowest order solution for  $\langle r(t) \rangle$  in Eqs. (62) and (63) is equivalent to the deterministic solution, given a known mean history  $\langle r_\tau(t) \rangle$ . The correction to the mean is proportional to  $\frac{\partial^2 v}{\partial r^2} \langle \Delta r^2 \rangle$ , which is strictly positive in the case of Eqs. (1)-(3).

The terms on the r.h.s. of Eq. (63) have simple interpretations. Supposing that the set of histories used in Eq. (63) contained only a single history, the terms proportional to  $v(r)$  vanish and only the term proportional to  $B(r)$  remains. This  $B(r)$  term is a standard diffusive term that arises in non-delayed theories. We label the contribution to  $\langle \Delta P^2 \rangle$  from such  $B(r)$  integrals the *Poisson-like contribution*, for reasons that will become clear. The integrated form of the diffusive term can be written as

$$\begin{aligned} \langle \Delta r(t)^2 \rangle_{\text{diffusion}} &\equiv \int_{t_i}^t dt' B(\langle r_\tau(t') \rangle) = \int_{t_i}^t dt' (F(\langle r_\tau(t') \rangle) + \gamma_r) \\ &\approx \langle r(t) \rangle - \langle r(t_i) \rangle + 2\gamma_r(t - t_i), \end{aligned} \quad (64)$$

where we used the lowest order approximation for  $\langle r(t) \rangle$  from Eq. (62). Equation (64), applied to the time of the production phase when  $r > 0$ , leads to the Poisson-like contribution

$$\langle \Delta P^2 \rangle_{\text{Poisson-like}} = \langle P \rangle + 2\gamma_r T_{P,r>0}, \quad (65)$$

where  $T_{P,r>0} \approx 2\tau$  is the time when the repressor is above zero during production phase. Since  $\langle P \rangle$  is typically of order  $(\alpha - \gamma_r)\tau$ , and  $2\gamma_r T_{P,r>0}$  is of order  $4\gamma_r\tau$ , for small  $\gamma_r/\alpha$  the last term can be neglected, and  $\langle \Delta P^2 \rangle_{\text{Poisson-like}} \approx \langle P \rangle$ .

That is, the diffusive term leads to a term reproducing the Poisson relationship between mean and variance. From the results in Section IV A, dominance of the Poisson-like term leads to the period variance

$$\langle \Delta T^2 \rangle_{\text{Poisson-like}} = \frac{2 \langle P \rangle}{\gamma_r^2}. \quad (66)$$

The remaining terms on the r.h.s. of Eq. (63) provide the *amplified noise contribution* to  $\langle \Delta P^2 \rangle$ . Unlike the Poisson-like contribution, Eq. (65), the amplified noise contribution depends sensitively on the variability of  $r(t)$  when  $r(t) < C_0$ , i.e. on how the pulse is created. Amplified noise allows the period variance to remain relatively large even when  $\langle P \rangle$  is large.

## 2. Delayed production from the degradation phase

To determine the variability of the amplitude and period, we integrate in stages, as was done for the deterministic case. All random repressor trajectories  $r(t)$  are synchronized by the condition that time  $t_0$  is the first time that repressor reaches zero at the end of the degradation phase, i.e.  $r(t_0) = 0$ . Thus, all trajectories  $r(t)$  converge at time  $t_0$  but generally diverge at other times.

The trajectories  $r(t)$  for times  $t < t_0$  are part of the degradation phase, and these trajectories may be used to sample  $r(t)$  at future times. These trajectories are approximately degrading at the constant rate  $K_- = \gamma_r$  when  $\gamma_r \tau \gg r_{\text{on}}$ . We assume that production is negligible in this phase, i.e.  $K_+ \approx 0$ . The trajectories with these conditions can be generated by the backwards Master equation [7]. This is done in conjunction with the boundary condition  $r(t_0 - \epsilon) = 1$ , where  $\epsilon$  is an infinitesimal positive time. This boundary condition is due to the transition of state  $1 \rightarrow 0$  occurring at time  $t_0$ . The probability distribution for the backwards-generated trajectories  $r(t)$  have a shifted Poisson distribution

$$\text{Probability}[r(t) = n + 1] = e^{\gamma_r t} \frac{(-\gamma_r (t - t_0))^n}{n!}, \quad t < t_0. \quad (67)$$

These trajectories have the approximate statistics (neglecting the shift of one repressor in the mean)

$$\langle r(t) \rangle = -\gamma_r (t - t_0) \quad (68)$$

$$\langle \Delta r^2(t) \rangle = -\gamma_r (t - t_0) \quad (69)$$

$$\kappa(r(t_2), r(t_1)) = \langle \Delta r^2(\max(t_1 - t_0, t_2 - t_0)) \rangle. \quad (70)$$

The correlation function, Eq. (70) is characteristic of diffusive fluctuations, except that the function depends on  $\max(t_1, t_2)$  rather than  $\min(t_1, t_2)$ , due to Eq. (67) arising from a backwards equation.

Like the deterministic system, the stochastic system during times  $t_0 \leq t \leq t_{\text{on}} + \tau$  does not tend to rapidly increase away from zero, with  $t_{\text{on}}$  defined by  $\langle r(t_{\text{on}}) \rangle = r_{\text{on}}$ . Thus, Eqs. (62) and (63) cannot be used for times in the range  $t_0 \leq t \leq t_{\text{on}} + \tau$ . However, during times substantially before  $t_{\text{on}} + \tau$ ,  $r(t)$  remains small and fluctuates near  $r = 0$ . For simplicity of our calculations, we extend the approximation  $r(t) = 0$  to the entire interval  $t_0 \leq t \leq t_{\text{on}} + \tau$ . Further comments on the  $r = 0$  approximation appear in Section IV B 3. Similarly, Eqs. (62) and (63) cannot be applied to generate statistics of  $r(t)$  for times just beyond  $t_{\text{on}} + \tau$ , i.e. before the probability  $p_0(t) \approx 0$ . We instead suppose for simplicity that Eqs. (62) and (63) can be applied precisely for times  $t_{\text{on}} + \tau \leq t$ , with  $r(t_{\text{on}} + \tau) = 0$ . Thus, two matched asymptotic approximations for  $r(t)$  are joined at the time  $t = t_{\text{on}} + \tau$ .

With the above assumptions, Eqs. (68)-(70) can be substituted into Eq. 63 to derive

$$\langle \Delta r_{\text{diffusion}}^2(t_0 + \tau) \rangle = \int_{t_{\text{on}}}^{t_0} dt (F(r(t)) + \gamma_r) = C_0 \left( \frac{\alpha}{\gamma_r} - 1 \right). \quad (71)$$

The full variance due to production during the degradation phase, including all contributions in Eq. (63), includes integrations over the correlation function, Eq. (70). The repressor variance at time  $t_0 + \tau$  is then

$$\langle \Delta r^2(t_0 + \tau) \rangle = \frac{C_0}{3} \left( \left( \frac{\alpha}{\gamma_r} \right)^2 - 3 \frac{\alpha}{\gamma_r} + 8 \sqrt{\frac{\alpha}{\gamma_r}} - 6 \right). \quad (72)$$

The correlation function for times  $t_{\text{on}} + \tau \leq t \leq t_0 + \tau$  can also be derived using Eq. (63), but the results are cumbersome and not reproduced here.

### 3. Delayed production from the principal production phase

The principal production phase, which occurs for times  $t_0 \leq t < t_{\text{on}} + \tau$ , tends to have rates that satisfy the inequality  $K_+(t) < K_-(t)$ . In the deterministic system, this inequality implies  $r(t) = 0$  until the time  $t_{\text{on}} + \tau$ . Using the same approximation as in Sec. IV B 2, suppose that  $r(t) = 0$  during times  $t_0 \leq t < t_{\text{on}} + \tau$ . Equations (62) and (63) then imply

$$\langle \Delta r^2(t_{\text{on}} + 2\tau) \rangle - \langle \Delta r^2(t_0 + \tau) \rangle = (\alpha + \gamma_r)(t_{\text{on}} + \tau - t_0). \quad (73)$$

The contribution to the burst magnitude variability (and, correspondingly, to the period variability) described by Eq. (73) is purely Poisson-like. This contribution is dominant in the limit  $C_0 \rightarrow 0$ , when production is binary with respect to  $r(t)$  (rate  $\alpha$  when  $r(t) = 0$ , rate 0 otherwise).

Though finite fluctuations in the stochastic system during the times  $t_0 \leq t < t_{\text{on}} + \tau$  are not used in the calculation of  $\langle \Delta P^2 \rangle$ , these fluctuations can become especially large near the time  $t_{\text{on}} + \tau$ . We have not found a simple way to estimate production variability arising near the time  $t_{\text{on}} + \tau$ , but fluctuations for times significantly before  $t_{\text{on}} + \tau$  can be estimated by approximating  $r(t)$  with a quasi-stationary system, i.e. a system with a sufficiently short characteristic correlation time. We do not analyze the quasi-stationary approximation here.

### 4. Delayed production from the times $t_{\text{on}} + \tau \leq t \leq t_{\text{on}} + 2\tau$

The methods in Sec. IV B 2 and IV B 3 lead to an approximate solution (in terms of elementary functions) for the mean and correlation function of  $r(t)$  for the times  $t_{\text{on}} + \tau \leq t \leq t_{\text{on}} + 2\tau$ , with the primary limiting assumption related to the matched asymptotic approximations for  $r(t)$  at the time  $t_{\text{on}} + \tau$ . The mean and correlation function of  $r(t)$  for times  $t_{\text{on}} + 2\tau \leq t \leq t_{\text{on}} + 3\tau$  can be found as before with Eqs. (62) and (63), and  $\langle \Delta P^2 \rangle \equiv \langle \Delta r(t_{\text{on}} + 3\tau) \rangle$  can in this way be expressed in terms of nested integrals (with a maximum of two dimensions of integration) over known functions of time. These nested integrals were done numerically for the results of this paper.

## C. Comparison of analytic results to numerical simulations

The above calculations for  $\langle \Delta r(t)^2 \rangle$ , conditional on synchronization at  $t = t_0$ , can be compared to averages derived directly from Gillespie simulations. Fig. 2b does this for a choice of parameters leading to a significant amplified noise contribution to  $\langle \Delta P^2 \rangle$ . Most of the Poisson-like variability appears as a linear ramp in  $\langle \Delta r(t)^2 \rangle$  during times  $t_0 + \tau \leq t \leq t_{\text{on}} + 2\tau$ . Amplified noise contributions are significant during times  $t_{\text{on}} + \tau \leq t \leq t_0 + \tau$  and  $t_{\text{on}} + 2\tau \leq t \leq t_0 + 2\tau$ , though Poisson-like contributions also reside here. The dominant amplified noise contribution to  $\langle \Delta r(t)^2 \rangle$  occurs at the end of a repressor burst near  $t = t_{\text{on}} + 2\tau$ . For times roughly in the range  $t > t_0 + 2\tau$ ,  $\langle \Delta r(t)^2 \rangle$  tends to be slowly changing, due to the onset of the degradation phase of the pulse.

Comparison between analytical and numerical results, such as in Figure 2, suggests that our matching of asymptotic approximations valid for  $t < t_{\text{on}} + \tau$  and  $t > t_{\text{on}} + \tau$  can lead to the prediction of low-order statistics for repressor dynamics. Deviation of the derived analytic results from the true results can arise from a number of factors. For instance, failure of Equations (68)-(70) to hold may occur when  $\gamma_r \tau \sim r_{\text{on}}$ , and this failure will lead to an error in our stochastic and deterministic analytic calculations.

## V. COMMENTS ON THE USE OF A PIECEWISE-LINEAR HILL FUNCTION

A simple model that reproduces many of the features of the stochastic system defined by Equations (1)-(3), is obtained when the Hill function in those equations is replaced by the piecewise linear function

$$F(r) = \begin{cases} \alpha \left(1 - \frac{2r}{C_0}\right) & , \quad 0 \leq r < \frac{C_0}{2} \\ 0 & , \quad r > \frac{C_0}{2}. \end{cases} \quad (74)$$

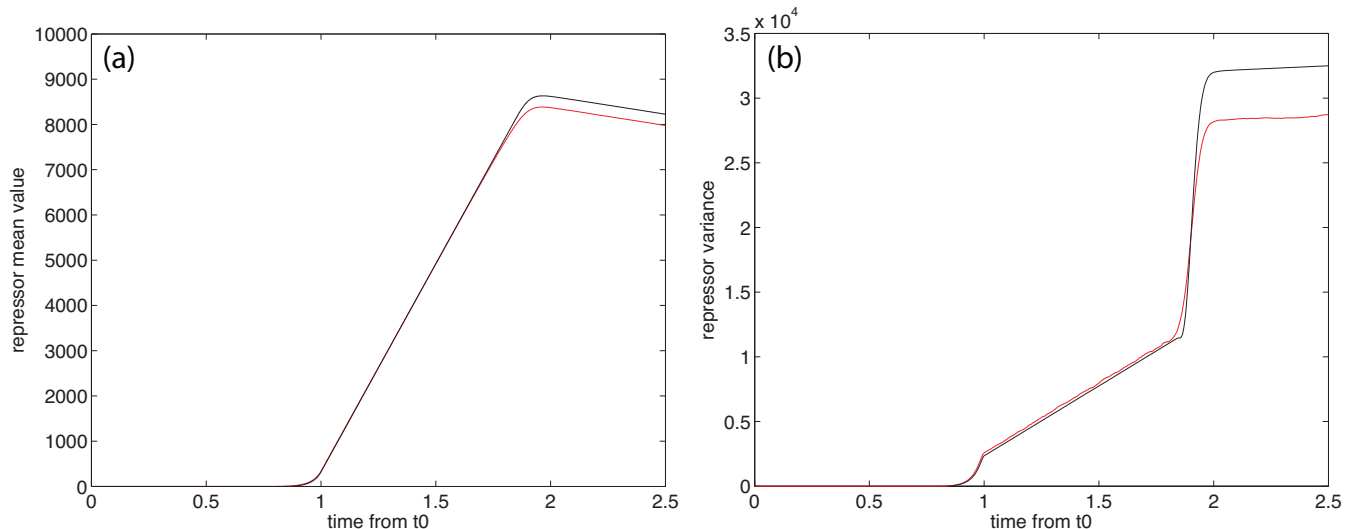


FIG. 2: Results from Gillespie simulations are compared to analytical results. Trajectories  $r(t)$  from Gillespie simulations are synchronized by the time  $t_0$  when  $r(t_0) = 0$  first occurs. (a) Comparison between the mean  $\langle r(t) \rangle$  obtained from Gillespie simulations (red) and analytic estimates for the deterministic trajectory (black). (b) The variance  $\langle \Delta r^2(t) \rangle$  from the same Gillespie simulations (red) and the small-noise expansions for the variance (black). The parameters used are  $\alpha = 10\,000$ ,  $\gamma = 800$ ,  $C_0 = 50$ ,  $\tau = 1$ . The stochastic results are derived from 4000 periods.

This model allows most of the preceding analytical results to be cast in terms of simple expressions, though we do not present the closed form of these results here. Notice that the omnipresent terms  $\frac{\partial v}{\partial r}$  in the small-noise approximations of  $r(t)$  are piecewise-constant

$$\frac{\partial v}{\partial r}(r) = \frac{\partial F}{\partial r}(r) = \begin{cases} -\frac{2\alpha}{C_0} & , \quad 0 < r < \frac{C_0}{2} \\ 0 & , \quad r > \frac{C_0}{2} \end{cases} \quad (75)$$

such that the integrals over  $\frac{\partial v}{\partial r}$  terms in Eqs. (62)(63) are proportional to integrals over correlation functions. We find in this simplified system, like in the original system, that ‘‘amplified noise’’ can significantly contribute to the pulse amplitude variability.

## VI. COUPLED POSITIVE-NEGATIVE FEEDBACK DF OSCILLATOR

While it appears that delayed negative feedback is the primary mechanism behind the oscillations observed experimentally in Ref. [3], the circuit built in that study also contained a positive feedback. Furthermore, when the positive feedback was removed, the circuit still oscillated - though with a smaller amplitude and less regular period. It appears that the positive feedback loop, though apparently non-essential for the production of oscillations, is regularizing the periods and making them more robust. The computational model reported in Ref. [3] suggests that delay in the positive feedback loop is less than in the negative feedback loop. The reasons for this are unknown, but may involve differences in transcription and/or translation rates, or the fact the functional form of the protein involved in the positive feedback loop, AraC, is dimeric, whereas LacI (the protein responsible for negative feedback) is functional in a tetrameric form.

The model (4)-(8) can be used to analyze the effect an additional positive feedback loop on the negative feedback-only system (1)-(3). The deterministic and stochastic variants of this model are briefly discussed in the following sections. The assumptions  $\beta = 0$  and  $R_0 \rightarrow 0$  are made for simplicity.  $f \geq 1$  is assumed.

The addition of positive feedback in Eqs. (4)-(8) implies that repressor is produced at the basal rate  $\alpha/f$  in the absence of activator, while repressor is produced at the higher activated rate  $\alpha$  in the presence of large quantities of activator. Recall from the discussion in Section III that the NFB system tends towards weak and noisy oscillations for large values of  $\alpha$ . In contrast, lower values of  $\alpha$  were associated with robust oscillations with repressor troughs at  $r = 0$ . This trend was tied to the failure of the strong inequality  $\gamma_r \tau \gg r_{\text{on}}$ . The addition of positive feedback effectively

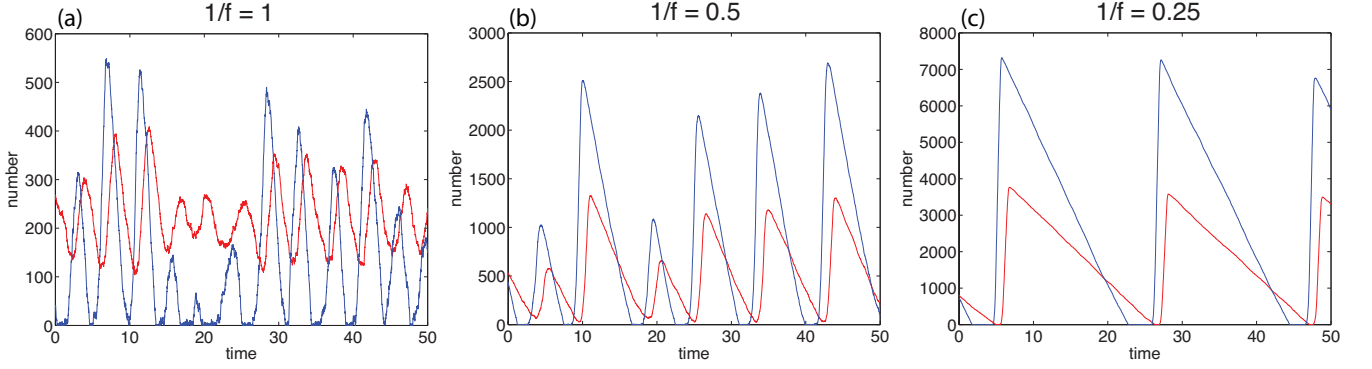


FIG. 3: Trajectories of repressor  $r(t)$  (red) and activator  $a(t)$  (blue) for the PNFB system (4)-(8). Parameters used are  $\tau = 1$ ,  $\tau_a = 0$ ,  $\alpha = 5000$ ,  $\gamma_r = 200$ ,  $\gamma_a = 440$ ,  $k = 2.0$ ,  $C_0 = C_1 = 50$ ,  $\beta = 0$ ,  $R_0 \rightarrow 0$ . (a)  $1/f = 1$ , i.e. no positive feedback. A sufficiently large value of  $\alpha$  is chosen, such that the NFB system undergoes weak oscillations, and the troughs for  $r(t)$  are above zero on average. (b)  $1/f = 0.5$ . In this case, repressor is produced at the lower basal rate  $\alpha/f$  until activator is produced. This allows  $r(t)$  to reach lower-valued troughs before production begins, leading to larger amplitude oscillations. (c)  $1/f = 0.25$ . The effect seen in (b) is more pronounced in (c).

reduces  $\alpha$  in the degradation phase of repressor, reducing the value  $r_{\text{on}}$  associated with the degradation phase of repressor, and permitting strong oscillations of repressor. Thus, the addition of positive feedback can stabilize weak NFB oscillations. Fig. 3 presents several sample trajectories of the PNFB system that demonstrate this effect.

### A. Deterministic analysis and results

PNFB oscillations are here analyzed in the deterministic case. Two conditions are imposed on the dynamics. Activator  $a(t)$  is assumed to reach troughs  $a = 0$  well before repressor approaches zero. This is approximately true when  $k/\gamma_a < 1/\gamma_r$ . The condition  $\gamma_a < k\alpha/f$  is assumed, such that activator, once at zero, can again increase away from zero.

A typical PNFB oscillation can be understood in terms of the NFB system with a time-dependent maximum production rate  $\alpha(t) = \alpha((1/f) + a(t)/C_1)/(1 + a(t)/C_1)$ .  $\alpha(t)$  varies between its basal and activated values  $\alpha/f$  and  $\alpha$ , respectively. In this case, we can show that activator begins to be produced at a time  $t_{\text{on},a} + \tau_a$  after the condition  $r(t_{\text{on},a}) = r_{\text{on},a}$  is satisfied, where

$$r_{\text{on},a} \equiv C_0 \left( \sqrt{\frac{k\alpha}{f\gamma_a}} - 1 \right). \quad (76)$$

If we assume  $C_1 \rightarrow 0$  (i.e. the activator switches on rapidly relative to changes in repressor) then

$$\alpha(t) \approx \begin{cases} \frac{\alpha}{f} & , \quad t \leq t_{\text{on},a} + \tau_a \\ \alpha & , \quad t > t_{\text{on},a} + \tau_a. \end{cases} \quad (77)$$

The piecewise approximation Eq. (77) for  $\alpha(t)$  can be substituted directly for  $\alpha$  in the previous theory for the NFB system. The integrals using a step function  $\alpha(t)$  are functionally no more complicated than in the NFB analysis.

Fig. 4 compares the  $C_1 \rightarrow 0$  theory to numerical integration of the delay differential equation derived from Eqs. (4)-(8). For the small value used,  $C_1 = 1$ , analytical results are primarily limited by the assumption that  $\dot{r} = -\gamma_r$  during the degradation phase of oscillations. Deterministic results for  $C_1 = 50$  are qualitatively similar to those for  $C_1 = 1$ , though analytical results do not match as well quantitatively for  $C_1 = 50$  as  $C_1 = 1$ .

This theory can be used to explain why the PNFB system has a reduced amplitude relative to the NFB system when  $\gamma_r\tau \gg r_{\text{on}}$  holds and  $\tau_a > 0$ . Suppose the limit  $C_0 \rightarrow 0$ , such that production of repressor and activator only occurs at the times  $t_0 + \tau$  and  $t_0 + \tau_a$ , respectively, where  $t_0$  is the time when  $r = 0$  first in an oscillation. For the PNFB system with  $0 \leq \tau_a \leq \tau$ , the amplitude  $P_r$  of a pulse of repressor is composed of pieces due to basal and activated

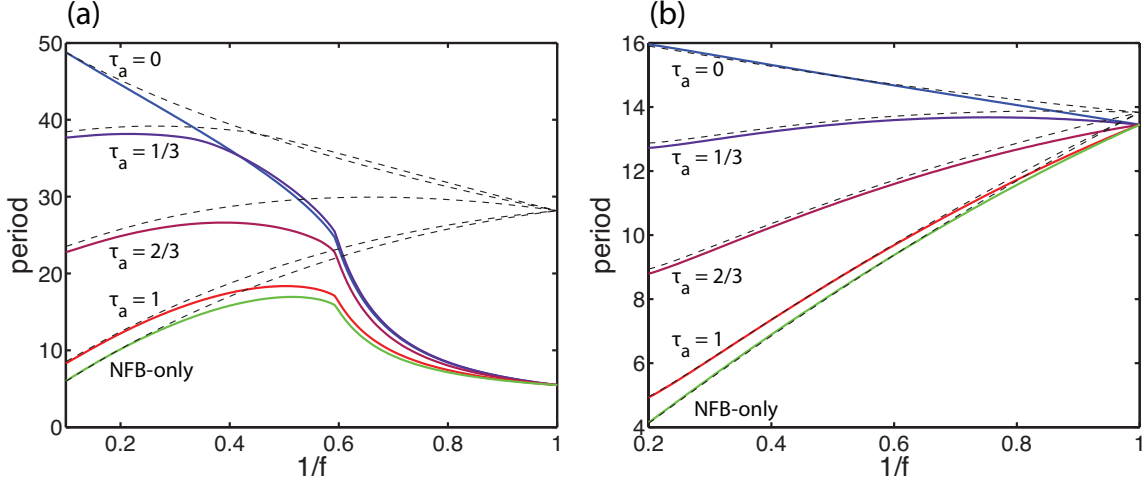


FIG. 4: Results of the deterministic coupled positive-negative feedback system, similar to Fig. 4 in the main text. (a) Period vs.  $1/f$  for different values of activator delay  $\tau_a$  (labeled in the plot). These results are compared to the negative feedback-only system (NFB) with the basal rate  $\alpha/f$  for the value of  $f$  on the abscissa. In this case, the activated rate is  $\alpha = 20000$ . As in Fig. 4 of the main text, oscillations reach a trough  $r = 0$  when approximately  $1/f < 0.6$ . Dashed lines are analytic results for the same set of parameters, with results matching their numerical counterparts when  $f$  is large. (b) The same as in (a), but with the lower activated rate  $\alpha = 6000$ . Other parameters used are  $\gamma_r = 400$ ,  $\gamma_a = 1200$ ,  $\tau = 1$ ,  $C_0 = 50$ ,  $C_1 = 1$ ,  $k = 2$ ,  $R_0 \rightarrow 0$ ,  $\beta = 0$ . A small value for  $C_1$  was chosen such that the theory in Sec. VIA agrees with results.

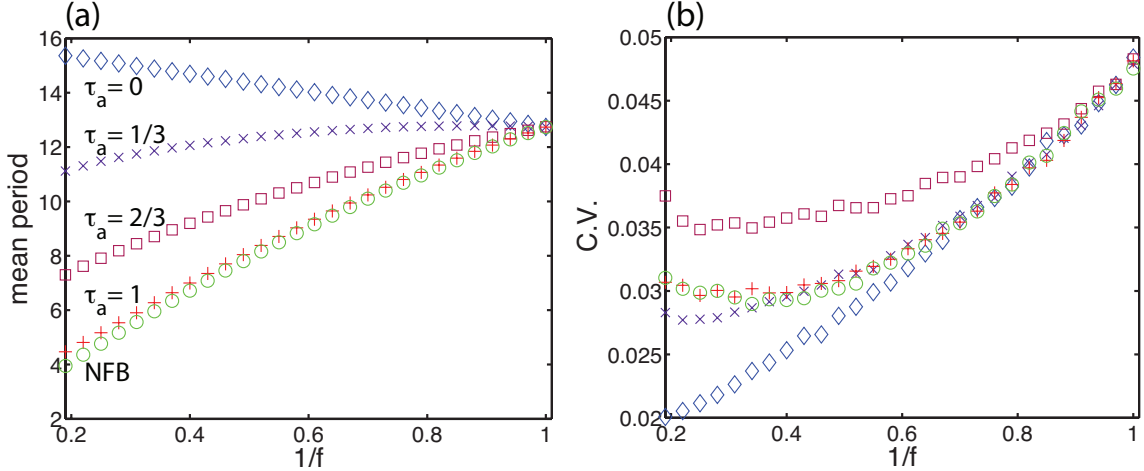


FIG. 5: Results of the stochastic oscillator, similar to Fig. 4 in the main text. (a) Mean period vs.  $1/f$  for different values of activator delay  $\tau_a$  (labeled in the plot), with the activated rate  $\alpha = 6000$ . These results are compared to the negative feedback-only system (NFB) with the basal rate  $\alpha/f$  for the value of  $f$  on the abscissa. (b) Coefficient of variability (C.V.)  $\sqrt{\langle \Delta T^2 \rangle} / \langle T \rangle$ , i.e. the period standard deviation divided by the mean period. The value of  $\tau_a$  is derived from the symbols in part (a). Other parameters used are  $\gamma_r = 400$ ,  $\gamma_a = 1200$ ,  $\tau = 1$ ,  $C_0 = 50$ ,  $C_1 = 50$ ,  $k = 2$ ,  $R_0 \rightarrow 0$ ,  $\beta = 0$ . Each point represents 10 000 period samples.

production

$$P_r = \left( \frac{\alpha}{f} - \gamma_r \right) \tau_a + (\alpha - \gamma_r)(\tau - \tau_a). \quad (78)$$

$P_r$  achieves a maximum value at  $\tau_a = 0$ . Since these oscillations have period  $T = 2\tau + P_r/\gamma_r$ , the period also has a maximum at  $\tau_a = 0$ . Thus, positive feedback does little to enhance oscillations in the  $C_0 \rightarrow 0$  limit. Compare this to the case in Fig. 4a, which is far removed from the  $C_0 \rightarrow 0$  limit.

## B. Stochastic results of the PNFB system

Addition of PFB also affects period variability in the stochastic system. The  $C_1 \rightarrow 0$  theory in Section VIA may also be used for the analysis of period variability, though this is not done here. Instead, we comment on numerical results.

Period variability for the PNFB system is partially explored in Fig. 3 of the main text, where the C.V. of the period for the PNFB system with high  $f$  was seen to be small relative to a NFB system with comparable amplitude. Numerical results from this Fig. 3 also demonstrated that the C.V. for different values of  $\tau_a$  but fixed  $f$  were similar to one another and comparable to the C.V. of the NFB system with basal rate  $\alpha/f$ . A different parameter regime from Fig. 3 of the main text uses a lower value for the activated rate  $\alpha$ , such that the negative feedback-only system has pronounced oscillations and troughs  $r = 0$ . Fig. 5 demonstrates that adding positive feedback to this system often *reduces* mean period and *increases* period C.V. as  $\tau_a$  grows larger than zero. The  $\tau_a = 0$  case continues to demonstrate increased mean period and lowered C.V.

- 
- [1] D. T. Gillespie, J. Phys. Chem. **81**, 2340 (1977).
  - [2] D. Bratsun, D. Volfson, L. S. Tsimring, and J. Hasty, Proc. Natl. Acad. Sci. USA **102**, 14593 (2005).
  - [3] J. Stricker et al., Nature (to be published) (2008).
  - [4] M. C. Mackey and I. G. Nechaeva, Phys. Rev. E **52**, 3366 (1995).
  - [5] A. C. Fowler and M. C. Mackey, Siam Journal On Applied Mathematics **63**, 299 (2002).
  - [6] M. B. Elowitz, A. J. Levine, E. D. Siggia, and P. S. Swain, Science **297**, 1183 (2002).
  - [7] C. Gardiner, *Handbook of Stochastic Methods* (Springer-Verlag, New York, 2004).